

Jamming under tension in polymer crazes

Jörg Rottler and Mark O. Robbins

Department of Physics and Astronomy, The Johns Hopkins University, 3400 N. Charles Street, Baltimore, Maryland 21218
(October 31, 2018)

Molecular dynamics simulations are used to study a unique expanded jammed state. Tension transforms many glassy polymers from a dense glass to a network of fibrils and voids called a craze. Entanglements between polymers and interchain friction jam the system after a fixed increase in volume. As in dense jammed systems, the distribution of forces is exponential, but they are tensile rather than compressive. The broad distribution of forces has important implications for fibril breakdown and the ultimate strength of crazes.

PACS numbers: 61.43.Fs, 62.20.Fe, 83.10.Rs

The common features of jammed systems ranging from molecular glasses to granular media have sparked great interest [1,2]. These systems jam as the available volume becomes too small to allow relative motion of particles. Unifying features of the jammed state are the presence of an exponential force tail at large *compressive* forces and the appearance of a network of forces on scales much larger than the size of the constituent molecules or grains [3,4]. The origins of these features are still debated.

In this Letter, we consider a qualitatively different jammed state that forms under *tension*. Many amorphous polymers expand from a typical dense glass to a “craze” consisting of a network of fibrils and voids [5]. As shown in Fig. 1, the dense and expanded jammed states coexist at a fixed tensile stress S , much like liquid and gas phases coexist at a fixed pressure. There are no covalent bonds that keep the craze from unravelling, but experiments suggest that the topological constraints called entanglements that limit dynamics in polymer melts behave like crosslinking bonds [5]. These experiments cannot address how deformation occurs, the distribution of forces within the system, or the configurations of individual chains within the intricate craze structure. We describe extensive molecular dynamics simulations that address all of these issues. We find that the distribution of tensile forces in the craze has an exponential tail analogous to that observed for compressive forces in dense jammed systems. The polymer undergoes an approximately affine displacement as it deforms into the craze. Expansion stops when segments that are only 1/3 of the distance between entanglements are pulled taut. This factor can be understood from simple geometric arguments and the assumption that entanglements act like chemical crosslinks between chains.

We study a standard coarse-grained model [6], where each linear polymer is modeled by N beads of mass m . Van der Waals interactions are modeled with a standard 6-12 Lennard-Jones (LJ) potential with energy scale ϵ and length scale σ . A simple analytic potential [7,8] is used for covalent bonds, with equilibrium length $l_0 = 0.96\sigma$ between adjacent beads along the

chain. In this fully flexible (fl) model, the number of beads between entanglements (entanglement length) is $N_e^{\text{fl}} \approx 70$ [6]. In order to analyze entanglement effects, we also consider semiflexible chains (sfl) where an additional bond-bending potential stiffens the chain locally and reduces the entanglement length to $N_e^{\text{sfl}} \approx 30$ beads [8–10]. We consider two temperatures $T = 0.1\epsilon/k_B$ and $T = 0.3\epsilon/k_B$, where the latter is close to the glass transition temperature. The strength of adhesive interactions between beads is varied by truncating the LJ force at either $r_c = 1.5\sigma$ or $r_c = 2.2\sigma$ [11].

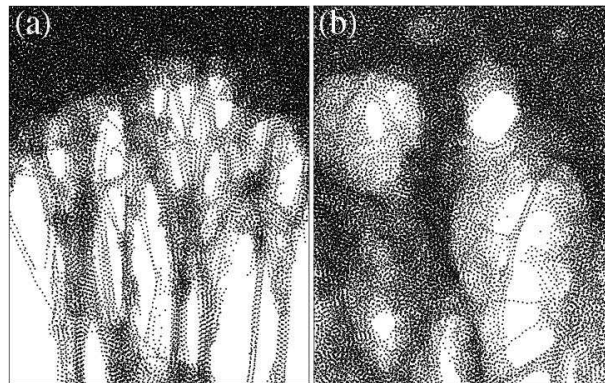


FIG. 1. Close-ups of interface between dense polymer and craze for (a) $T = 0.1\epsilon/k_B$, $r_c = 1.5\sigma$ (fl) and (b) $T = 0.3\epsilon/k_B$, $r_c = 2.2\sigma$ (sfl). The lateral dimension of both panels is 64σ . The diameter and spacing of the fibrils increase as T and/or r_c increase.

An amorphous glassy state is created in a cubic simulation cell of side L using standard techniques [6]. The period in the z -direction is then increased at a small constant velocity [11]. After an initial nucleation period, the system separates into two phases (Fig. 1). The craze network grows at constant tensile stress S through plastic flow in a narrow interfacial region called the “active zone.” The volume occupied by the polymer increases by an “extension ratio” λ that is remarkably insensitive to all parameters other than N_e . For example, increasing the temperature and interaction range leads to much

larger fibrils in Fig. 1(b) than (a), yet there is no measurable change in λ . From the ratios of the initial and final densities we obtain $\lambda_{\text{fl}} = 6.0 \pm 0.6$ and $\lambda_{\text{sfl}} = 3.5 \pm 0.3$, independent of N , T , and r_c . Experimental values of λ range from about 2 to 7 [5].

Although strain rate is strongly localized at the instantaneous position of the active zone, the net effect is a nearly uniform or affine expansion of each region of the polymer. As shown in Figure 2(a), the final height z_f of beads with an initial height of z_i is very close to λz_i . The rms variation in the final height (half the errorbar length), has a relatively small constant value. For reasons discussed below, it is close to $N_e/3$ for both flexible and semiflexible chains at all T and r_c studied. There are also much smaller rms displacements in the $x - y$ plane. These allow chains to lower their free energy by gathering into fibrils whose local density is close to that of the dense glass. The magnitude of lateral displacements varies with the size and spacing of fibrils, which depends on both T and r_c . For example, the lateral displacement increases from $\sim 2.5\sigma$ in Fig. 1(a) to $\sim 5.6\sigma$ in Fig. 1(b).

The affine nature of the deformation along z can also be inferred from the change in the conformation of individual polymers. In the initial state, chains exhibit an ideal random walk (RW) structure inherited from the melt. The rms distance $\Delta r(\Delta N)$ between beads that are ΔN neighbors apart scales as $\Delta r^2 = l_p l_0 \Delta N$, which defines the persistence length l_p . In the dense glass, the mean-squared projection along each of the three axes is equal. An affine deformation by λ along z will only change the displacements along the z -axis, yielding $\langle \Delta z^2 \rangle = \lambda^2 l_p l_0 \Delta N / 3$. Fig. 2(b) shows that the final conformation of chains follows this expression at large scales. The in-plane components of the displacement are not changed during crazing.

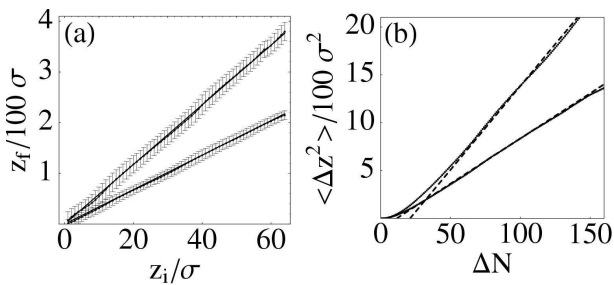


FIG. 2. (a) Final vs. initial height for flexible (large slope) and semiflexible (small slope) chains ($T = 0.1 \epsilon/k_B$, $r_c = 1.5\sigma$). Averages were performed over z -intervals of width σ . Straight lines have slope $\lambda_{\text{fl}} = 5.9$ and $\lambda_{\text{sfl}} = 3.5$, respectively. Error bars show the standard deviation from the averages at each height and are $17 \pm 1\sigma$ (fl) and $9 \pm 1\sigma$ (sfl). (b) Height change Δz as a function of distance ΔN from the chain center. Straight lines have slope $\lambda^2 l_p l_0 / 3$ with λ from (a). Systems at different T , r_c and N show the same results.

The expansion along z pulls short segments of the

chains taut, so that Δz^2 rises quadratically at small ΔN in Fig. 2(b). The typical number of beads in a taut segment, \tilde{N}_{st} , can be obtained from the intersection between the two asymptotic scaling forms: $(\tilde{N}_{\text{st}} l_0)^2 = \lambda^2 l_p l_0 \tilde{N}_{\text{st}} / 3$, yielding $\tilde{N}_{\text{st}} = \lambda^2 l_p / 3 l_0$. Inserting the observed values of λ and l_p ($l_p^{\text{fl}} = 1.65\sigma$ and $l_p^{\text{sfl}} = 2.7\sigma$), we arrive at $\tilde{N}_{\text{st}}^{\text{fl}} \simeq 21 \pm 4$ and $\tilde{N}_{\text{st}}^{\text{sfl}} \simeq 12 \pm 2$, respectively. The length of taut sections can also be determined by direct analysis of the chain geometry. Fig. 3(a) shows the distribution $P(N_{\text{st}})$ of the number N_{st} of successive beads whose displacement continues upwards or downwards. Here a bond is considered up (down) if it is within 45° of the $+z$ ($-z$) axis. For both flexible and semiflexible chains, $P(N_{\text{st}})$ has an exponential tail with a characteristic decay length that, like λ , is independent of N , T , and r_c . The decay lengths, $\tilde{N}_{\text{st}}^{\text{fl}} \sim 24 \pm 3$ and $\tilde{N}_{\text{st}}^{\text{sfl}} \sim 13 \pm 2$, are in good agreement with the prediction from RW statistics. Essentially the same length scales appear in the decay of the correlation function for the z -component of successive bonds, Fig. 3(b), or the bond-angle correlation function (not shown).

It is not surprising that all the above lengths are comparable to the deviations from a purely affine deformation in Fig. 2(a), since segments of length \tilde{N}_{st} are stretched taut from their initial RW configuration. However, a very successful expression for λ is usually derived by assuming that the taut segments contain N_e beads rather than $N_e/3$ [5]. The maximum extension ratio, λ_{max} , is defined as the ratio between the fully stretched length $N_e l_0$ and the initial end-to-end distance of a RW of N_e steps

$$\lambda_{\text{max}} \equiv N_e l_0 / (l_0 l_p N_e)^{1/2} = \sqrt{l_0 N_e / l_p}. \quad (1)$$

Calculated values of λ_{max} are very close to values of λ measured in experiments and in our simulations where $\lambda_{\text{max}} = 6.5 \pm 0.5$ and 3.5 ± 0.3 for flexible and semiflexible chains, respectively. However, it was noted in early work that fully stretched chains would actually yield an even larger extension ratio because the initial end-to-end vector of segments of length N_e is randomly oriented [12]. Since the mean-squared projection along any direction is only $1/3$ of the total, λ would be $\sqrt{3} \lambda_{\text{max}}$ for fully stretched chains. The observation that $\lambda \approx \lambda_{\text{max}}$ implies that the average length of stretched segments is only $N_e/3$, as we have shown. However those segments that are initially along the z -axis are fully stretched when $\lambda = \lambda_{\text{max}}$, and it appears that these few segments are sufficient to prevent further elongation. Thus the factor of $1/3$ results from the random nature of the entangled network. Note that a recent study of chains with random crosslinks [13] is consistent with Eq. (1), while all segments between crosslinks were fully stretched in a similar study of ordered networks [14].

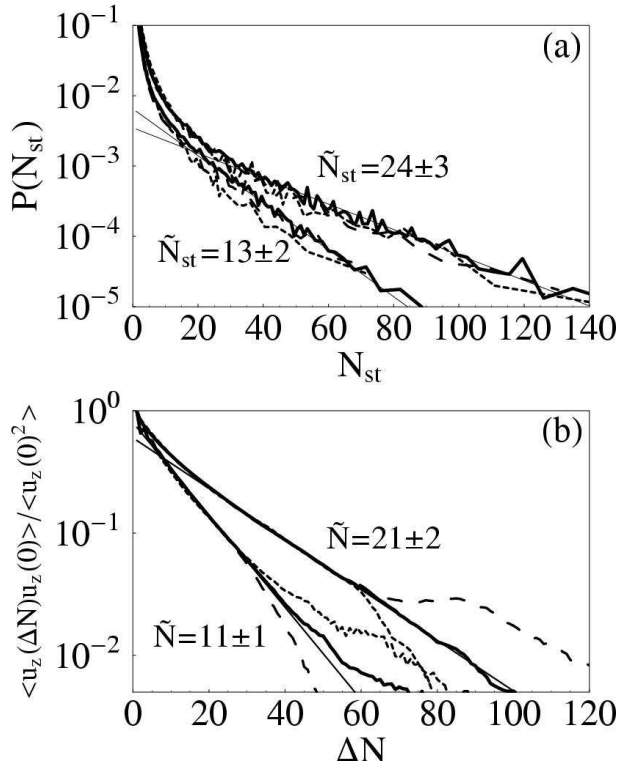


FIG. 3. (a) Probability of straight segments of length N_{st} for flexible and semiflexible chains. Thick lines: $T = 0.1 \epsilon/k_B$, $r_c = 1.5\sigma$, $N = 512$ and 1048576 beads. Dotted lines: $T = 0.3\epsilon/k_B$, $r_c = 2.2\sigma$, $N = 512$ and 262144 beads. Long dashed lines: $T = 0.1\epsilon/k_B$, $r_c = 1.5\sigma$, $N = 256$ and 262144 beads. (b) correlation function for the z -components of the bonds for the same systems. Thin solid lines in both panels show fits to an exponential decay with indicated decay lengths.

A crosslinked system will jam when there is a network of fully stretched covalent bonds, but it is less clear how entanglements can lead to a jammed network. The entanglement length is typically determined from the response of a polymer melt to a sudden strain [6,15]. The resulting time-dependent stress shows a broad plateau where the polymer has relaxed on short length scales, but is unable to relax at larger length scales because interpenetrating loops of polymer cannot pass through each other. The entanglement length corresponds to the typical length along the backbone between these constraints. The stress ultimately decays by the slow diffusion of polymers along their length until their ends pass through the loops and release all remaining constraints. Expansion of the polymer into a craze is also limited by the inability of polymer loops to pass through each other and interchain friction prevents the chains from unraveling by the snake-like motion that allows diffusion in the melt. The tension pulling two interpenetrating loops in opposite directions creates large compressive forces at the entanglements. As in conventional jammed systems this increases the barrier for sliding. Long chains have many interpenetrating loops,

and the tensions pulling in each direction nearly cancel. Chains with $N < 2N_e$ disentangle rather than forming a craze [11].

The distance between entanglements is determined by the chain statistics [16] which are inherited from the melt. They are not sensitive to temperature because there is no evolution of large scale structure in the glassy phase, and they are relatively insensitive to the strength of adhesive interactions and density. Thus λ is nearly constant, while the fibril structure at scales less than N_e may vary dramatically (Fig. 1). We have verified that λ only depends on chain statistics by artificially varying the persistence length l_p in the glassy state. As expected, the value of λ depends only on l_p and not on the flexibility of the chains, r_c , or other details of the interaction potential.

As in other jammed systems, the distribution of forces in the craze follows a universal curve with an exponential tail (Fig. 4). The tensions f in the covalent bonds along the chains carry most of the stress. Only 10-20% of covalent bonds are under compression ($f < 0$), and this part of the distribution does not change much during crazing. The tensile ($f > 0$) part of the distribution is exponential, and results for all systems collapse after normalizing by the average $\langle f \rangle$ over the tensile region. Intuitively, one might expect the crazes with the larger extension ratio (and N_e) to exhibit a larger average tension than the less stretched crazes. However, we find that $\langle f \rangle$ is a function of temperature T and cutoff range r_c only (see caption) and does not depend on N_e . Expanding the craze elastically beyond λ increases $\langle f \rangle$, but the normalized probability is unchanged until bonds begin to break.

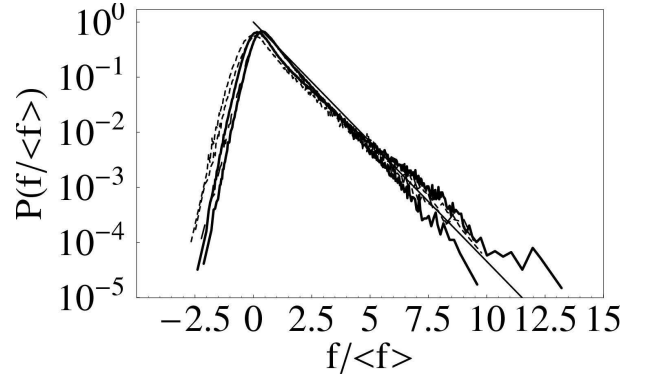


FIG. 4. Distribution of tension f in the craze for the systems of Fig. 3. The straight line is $\exp(-f/\langle f \rangle)$. Only bonds under positive tension were included in calculating $\langle f \rangle$. $\langle f \rangle \approx 8.2\epsilon/\sigma$ for $T = 0.3\epsilon/k_B$, $r_c = 2.2\sigma$, $\langle f \rangle \approx 7.2\epsilon/\sigma$ in all other cases.

In equilibrium, the energy of any region follows the exponential Boltzmann distribution because this maximizes the number of microstates available to the entire system at fixed total energy. In jammed systems the total force is conserved, and one may imagine that the exponential dis-

tribution of local forces also arises because it maximizes the number of microstates. Two more detailed models for the exponential distribution have been suggested for dense jammed systems.

The “q-model” [4] and its generalizations [17] assume that stress propagates unevenly through the system. The fraction of stress passed to each neighbor, q , is chosen at random from a distribution $R(q)$. For a wide range of R one obtains an exponential force distribution. In addition, the stress is concentrated in force chains like those seen in experiments on granular systems. The fibril network in a craze naturally provides a branching path for transmission of stress. Force is conserved along each fibril and then redistributed at the nodes where fibrils merge or split. Study of the stress along chains shows that tension is correlated along straight segments and then changes when the chain changes direction at a node. A more detailed comparison to the q-model is in progress.

Recently, O’Hern *et al.* [2] have proposed an alternative explanation for the exponential force tail in jammed materials. In equilibrium, the separation of beads at small distances is weighted by a Boltzmann-factor $\exp[-V(r)/k_B T]$, where $V(r)$ is the interaction potential. The corresponding distribution of forces is also nearly exponential if the force varies rapidly with r . The repulsive part of the LJ potential satisfies this criterion, but our covalent bond potential does not. We have calculated the distribution of bond energies in the craze and find that it is not exponential.

The presence of an exponential stress distribution has consequences for the ultimate fracture of craze fibrils. In a minimal model often employed in the literature [18], the maximum breaking force F_{\max} of a fibril composed of n strands is estimated by assuming that each strand carries an equal share of the load and all covalent bonds break at a critical force f_c . This implies $F_{\max}/f_c = n$, and all strands break at the same time. If the distribution of forces among strands is exponential, the most stressed strand will break at a lower F_{\max} . The force needed to initiate failure can be estimated using a simple scaling argument. The first strand will break when $nP(f > f_c) = n \int_{f_c}^{\infty} 1/\langle f \rangle \exp(-f/\langle f \rangle) df = n \exp(-nf_c/F_{\max}) = 1$, where we have used $\langle f \rangle = F_{\max}/n$. This implies a breaking force of $F_{\max}/f_c = n/\ln(n)$ instead of n . The redistribution of load after a strand breaks will cause the remaining strands to break sequentially. Note that no chain scission occurs in the simulations presented here, but it does occur upon further straining of the craze. A detailed analysis of fibril breakdown will be presented elsewhere.

In summary, we have shown that crazing transforms a conventional dense jammed state into a unique expanded jammed state. Expansion is limited by the same interlocking of polymer loops that leads to entanglements in polymer melts. However, the average length of straight

segments is only $N_e/3$ due to the random nature of the network. Interchain friction prevents disentanglement of the loops. As in dense jammed systems, the distribution of forces is exponential. However, the forces are tensile rather than compressive. We hope that contrasting this new jammed state with conventional ones will help unravel the microscopic origin of their common features.

This work was supported by the Semiconductor Research Corporation (SRC) and by the NSF grant No. DMR0083286. We thank E. J. Kramer, H. R. Brown, and C. Denniston for useful discussions.

-
- [1] A. J. Liu and S. R. Nagel (Eds.), *Jamming and Rheology*, (Taylor & Francis, London, 2001)
 - [2] C. S. O’Hern, S. A. Langer, A. J. Liu, and S. R. Nagel, *Phys. Rev. Lett.* **86**, 111 (2001)
 - [3] C.-h. Liu, S. R. Nagel, D. A. Schecter, S. N. Copper-smith, S. Majumdar, O. Narayan, T. A. Witten, *Science* **269**, 513 (1995)
 - [4] S. N. Coppersmith, C.-h. Liu, S. Majumdar, O. Narayan, and T. A. Witten, *Phys. Rev. E* **53**, 4673 (1996)
 - [5] E. J. Kramer, L. L. Berger, *Adv. Polymer Science* **91/92**, 1 (1990).
 - [6] M. Pütz, K. Kremer, G. S. Grest, *Europhys. Lett.* **49**, 735 (2000). The quoted N_e is from the plateau modulus.
 - [7] The potential is $V_{br}(r) = -k_1(r - r_c)^3(r - R_1)$, and the constants k_1 and R_1 are adjusted to fit the equilibrium bond length and to allow for bond breaking when the tension exceeds 100 times the breaking force f_{LJ} of the van der Waals bonds.
 - [8] S. W. Sides, G. S. Grest, M. J. Stevens, *Phys. Rev. E* **64**, 050802 (2001), *Macromolecules* **35**, 566 (2002).
 - [9] R. Faller, F. Müller-Plathe, and A. Heuer, *Macromolecules* **33**, 6602 (2000) and R. Faller and F. Müller-Plathe, *ChemPhysChem.* **2**, 180 (2001).
 - [10] The bond-bending forces are modeled with $V_B = \sum_{i=2}^{N-1} b \left(1 - \frac{(\vec{r}_{i-1} - \vec{r}_i) \cdot (\vec{r}_i - \vec{r}_{i+1})}{|\vec{r}_{i-1} - \vec{r}_i| |\vec{r}_i - \vec{r}_{i+1}|} \right)$, where \vec{r}_i denotes the position of the i th bead along the chain, and b characterizes the stiffness.
 - [11] A. R. C. Baljon, M. O. Robbins, *Macromolecules* **34**, 4200 (2001).
 - [12] E. J. Kramer, *Adv. Polymer Sci.* **52/53** 1 (1983).
 - [13] S. Barsky and M. O. Robbins, unpublished
 - [14] M. J. Stevens, *Macromolecules* **34**, 1411 (2001)
 - [15] M. Doi and S. F. Edwards, *The Theory of Polymer Dynamics*, (Oxford University Press, Oxford, 1986)
 - [16] L. J. Fetters, D. J. Lohse, D. Richter, T. A. Witten, and A. Zirkel, *Macromolecules* **27**, 4639 (1994)
 - [17] P. Claudin, J.-P. Bouchaud, M. E. Cates, and J. P. Wittmer, *Phys. Rev. E* **57**, 4441 (1998)
 - [18] R. A. L. Jones, R. W. Richards, *Polymers at Surfaces and Interfaces*, (Cambridge University Press, Cambridge, 1999).